ELSEVIER

Journal of Molecular Catalysis A: Chemical 121 (1997) 33–44

JOURNAL OF MOLECULAR CATALYSIS A: CHEMICAL

Effect of hydrogen reduction on the CO adsorption and methanation reaction over Ru/TiO_2 and Ru/Al_2O_3 catalysts

V.P. Londhe, V.S. Kamble, N.M. Gupta *

Chemistry Division, Bhabha Atomic Research Centre, Trombay, Mumbai-400085, India

Received 10 April 1996; accepted 15 November 1996

Abstract

The C–O stretch vibrational bands developed over Ru/TiO_2 and Ru/Al_2O_3 catalyst surfaces during adsorption of CO at different temperatures were investigated as a function of H_2 pretreatment given to a sample in the temperature range of 575–875 K. While the reduction at temperatures below 675 K had no significant effect, the higher temperature H_2 pretreatment resulted in the progressive annihilation of νCO bands in the 2050–2145 cm^{-1} region, identified with the multicarbonyl species bonded to Ru sites of different oxidation states. The removal of these bands showed a parallelism with the loss of catalyst activity at reaction temperatures below 500 K, whereas the activity at the temperatures above 550 K remained almost unaffected. We conclude that the $Ru(CO)_n$ species are formed over highly dispersed metal surfaces and are responsible to the low temperature catalytic activity. On the other hand, the catalytic activity at higher reaction temperatures is attributed to certain monocarbonyl moieties, the formation of which is rather independent of metal dispersion. Our results also reveal the occurrence of the reductive surface agglomeration of Ru metal at high temperatures and the reformation of the smaller crystallites on subsequent exposure of the catalyst to O_2.

Keywords: Adsorption; Carbon monoxide; Methanation; Ruthenium/titania; Ruthenium/alumina

1. Introduction

A number of vibrational spectroscopy studies using supported ruthenium catalysts have shown that the mode of adsorption of a simple molecule, such as CO, may depend upon various factors such as, the nature of the support, the metal dispersion, the temperature/pressure of the adsorbate and the presence of additives, such as H_2, O_2 and H_2O [1–16]. It is also well established now that a high temperature H_2 pretreatment affected CO adsorption and hydrogenation activity of supported noble metal catalysts, particularly when the support used was a reducible metal oxide (see reviews [17–19]). However, the individual $(CO)_{ad}$ modes influenced by H_2 pretreatment and their effect on the CO hydrogenation behaviour of a particular catalyst are not identified as yet. A recent study from our laboratory has revealed that the sulphur deposition over Ru/TiO_2 catalyst hinders the development of certain multicarbonyl and monocarbonyl species responsible to νCO bands in 2055–2140 cm^{-1} region which otherwise transform to methane via surface methylene

* Corresponding author. Fax: 91-22-5560750; e-mail: nmgupta@magnum.barct1.ernet.in

PII S1381-1169(96)00449-9

groups in the presence of chemisorbed hydrogen [20]. On the other hand, the $(CO)_{ad}$ species giving rise to lower frequency bands were affected to a lesser extent. Another study using scanning electron microscopy has shown that the hydrogen reduction at temperatures above 675 K led to the segregation and agglomeration of Ru over Ru/TiO_2 catalyst surface, which showed a strong parallelism with the loss of catalyst activity for the adsorption and hydrogenation reactions of CO [21]. In continuation, we now report the results of our FTIR spectroscopy study demonstrating the H_2 pretreatment effect on the CO binding states over title catalysts. Corresponding data on the CO hydrogenation activity of these catalysts are also given.

2. Experimental

2.1. Catalyst

Three different Ru catalysts having titania and alumina as supports were used in this study. The titania supported catalysts were prepared using coprecipitation method, starting with the chlorides of ruthenium and titanium and using a 20% ammonium bicarbonate solution for precipitation. The alumina based catalyst was prepared by impregnation of 60–100 mesh size γ-alumina with a ruthenium trichloride solution. All the samples were dried in air (350 K) followed by O_2 sintering (525 K, 16 h and 625 K, 8 h) and H_2 activation at 575 K for 2 h. The effect of H_2 pretreatment at higher temperatures was also evaluated. For this purpose, fresh lots of O_2 sintered samples were subjected to a 2 h treatment under $H_2 + Ar$ (1:1) flow (60 ml min^{-1}) at various temperatures in range 600–1000 K. The XRD analysis of Ru/TiO_2 samples showed that about 80% of titania existed in the anatase form, the rest being in rutile phase. While the metal content of different samples was determined by X-ray fluorescence method, the volumetric measurement of H_2 chemisorption was employed to evaluate the metal dispersion. The physical characteristics of the different samples used in this study are given in Table 1.

2.2. Activity measurements

A conventional quartz microcatalytic tubular reactor, operating in flow mode at 1 atm pressure was employed for evaluation of the catalyst activity in two different modes and at different reaction temperatures. In the flow mode, a $CO + H_2$ (1:4) gas mixture was passed (0.7 l h^{-1}) over 0.5 g of a catalyst and the sampled effluent was analysed at regular intervals using a gas chromatograph equipped with a thermal conductivity detector and a Porapak-Q column, both maintained at 300 K. In pulse mode, 100 μl (ca. 4.1 μmol) pulses of CO were introduced into H_2 carrier flowing over the catalyst bed and the reaction products were analysed using the GC connected on-line. The measurements under pulse mode provided the activity data of a fresh catalyst for comparison purposes, without any significant poisoning due to coke formation.

2.3. Infrared spectroscopy

A high pressure and high vacuum stainless steel cell used in this study has been described

Table 1
Details of Ru catalysts

Catalyst	Preparation method	Metal content wt.- %	Surface area $m^2\ g^{-1} \pm 5\%$	Dispersion (%)
1. Ru/TiO_2	Coprecipitation	2.2	91	12
2. Ru/TiO_2	Coprecipitation	4.3	90	10
3. Ru/Al_2O_3	Impregnation	4.5	140	5

earlier [13–15]. The cell has water cooled CaF_2 windows and permits in situ treatment to a sample at temperatures up to 625 K, either under a gas stream or under a vacuum of ca. 10^{-4} Torr. The sample (ca. 70 mg) was used in form of a self-supporting wafer of 25 mm diameter. A catalyst wafer reduced under H_2 at a particular temperature and cooled under argon flow was transferred to the IR cell with a minimum time delay. It was activated in situ at 473 K (2 h) followed by 2 h evacuation at 573 K. A background spectrum was recorded at this stage after cooling the sample to required temperature and before exposing it to a dose of CO.

In order to compensate for the presence of unadsorbed CO in the cell, the difference spectra were obtained by subtracting from sample spectrum the IR spectrum of a metal free titania disc recorded in the presence of a suitable pressure of CO. The overlapping vibrational bands were computationally resolved with the help of a Fourier self-deconvolution program in the spectrometer software using a suitable combination of following parameters: full width at half maximum (w), enhancement factor (k), fraction Lorentzian (f), and the apodization or smoothing function (a), as has been described earlier in detail [20].

A Mattson model Cygnus-100 FTIR spectrometer equipped with a DTGS detector was employed for this study. Normally 300 scans were recorded in the transmittance mode and at 4 cm^{-1} resolution for each spectrum.

Carbon monoxide of 99.9% purity from Airco (USA) was used after passing through a dry ice trap to remove any carbonyl or moisture impurities. H_2 was purified by passing through a deoxo catalyst and a molecular sieve trap.

3. Results

3.1. Catalyst activity

3.1.1. Pulse mode

Fig. 1 and Fig. 2 show the effect of H_2 pretreatment on the temperature dependent CO methanation activity of two of the catalyst samples studied in the pulse mode. In both the cases, the methane yield decreased drastically when a sample was subjected to a high temperature H_2 pretreatment, the effect being more pronounced on the catalyst activity at reaction temperatures lower than 570 K. The Ru/Al_2O_3

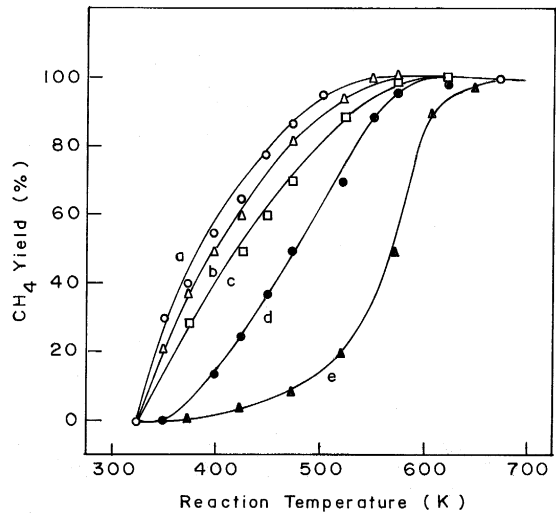

Fig. 1. The CO methanation activity of a $Ru(2.2\%)/TiO_2$ catalyst as a function of hydrogen pretreatment given to the sample at different temperatures. (a) 475 K, (b) 575 K, (c) 675 K, (d) 775 K and (e) 875 K.

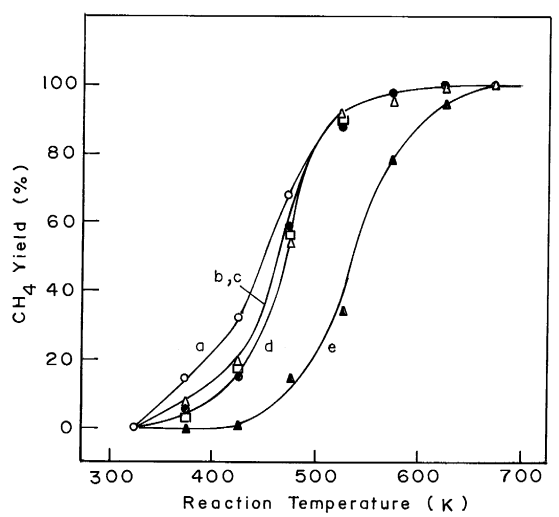

Fig. 2. The CO methanation activity of a $Ru(4.5\%)/Al_2O_3$ catalyst as a function of hydrogen pretreatment given to the sample at different temperatures. (a) 475 K, (b) 575 K, (c) 675 K, (d) 775 K and (e) 875 K.

catalyst showed comparatively poor activity but was more resistant to the hydrogen pretreatment and thus the substantial loss in catalyst activity was detected only after reduction at the temperatures greater than 750 K (Fig. 2). In the case of more active Ru/TiO_2 catalyst, the activity loss was observed after reduction at a temperature of 675 K or above (Fig. 1). Even though the trend was the same, the extent of the activity loss was smaller in the $Ru(4.3\%)/TiO_2$ sample as compared to the one having lower metal content. In each case, the activity was restored to an almost original value when a high temperature reduced sample was heated in O_2 (575 K, 2 h) and then subjected to H_2 activation under mild conditions (525 K, 2 h).

Data in Fig. 1 and Fig. 2 show that the methane yield was almost 100% during $CO + H_2$ reaction at the temperatures above 575 K, irrespective of the catalyst used and also irrespective of the pretreatment conditions. Maximum effect of high temperature pretreatment was detected for the reaction temperatures below 475 K. Thus, as compared to 87% CH_4 yield observed at a reaction temperature of 475 K using a 475 K reduced catalyst (Fig. 1a), only about 50% and 8% of CO was reacted to form CH_4 at this temperature when the reduction temperature was raised to 775 and 875 K, respectively (Fig. 1, curves d and e).

In addition to methane, a small amount of ethane was also formed using the titania supported catalysts. Furthermore, the yield of C_2H_6 also varied with the catalyst reduction temperature. Fig. 3 presents these data for a $Ru(2.2\%)/TiO_2$ sample. For the catalyst samples reduced at temperatures in the 475–675 K region, the ethane formation commenced at 370 K and reached a saturation value at a reaction temperature of ca. 450 K; the C_2H_6 yield decreasing again with the further rise in bed temperature (Fig. 3, curves a–c). However, the ethane formation commenced at progressively higher reaction temperatures with the increase in H_2 pretreatment temperature, as shown by curves d and e of Fig. 3.

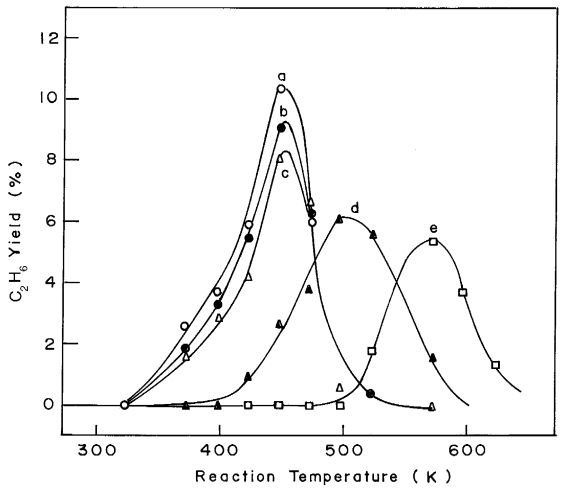

Fig. 3. C_2H_6 yields when 4.1 μmol CO pulses were reacted over a $Ru(2.2\%)/TiO_2$ catalyst at different temperatures under H_2 flow as a function of H_2 pretreatment given to the catalyst at different temperatures. (a) 475 K, (b) 575 K, (c) 675 K, (d) 775 K and (e) 875 K.

A part of the unreacted/unadsorbed CO was also eluted in effluents, the amount of which depended on the H_2 pretreatment condition and reaction temperature. Thus, no CO was evolved under studied reaction conditions when the $Ru(2.2\%)/TiO_2$ catalyst was subjected to H_2 pretreatments at the temperatures lower than 670 K. For the catalysts reduced at higher temperatures, a large fraction of unreacted CO was evolved, particularly at the lower reaction temperatures. For instance using a 770 K reduced sample, while ca. 75% of injected CO was eluted at the reaction temperatures below 400 K, almost a negligible amount of CO was released at the temperatures above 500 K, in agreement with the methane yields observed under this condition. With the further increase in reduction temperature to 875 K, the amount remaining unreacted was 90–100% at the sample temperatures below 420 K, the corresponding value being 55 and 30% for the reaction temperatures of 525 and 575 K.

No unreacted CO was, however, evolved using the Ru/Al_2O_3 sample irrespective of the reduction conditions and under the reaction temperatures of this study.

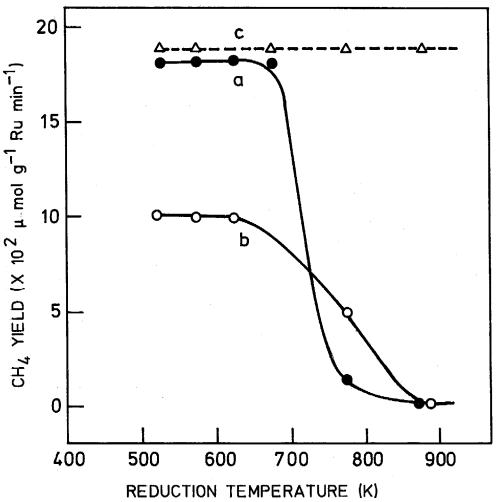

Fig. 4. The effect of reduction temperature on methane yields when $CO + H_2$ (1:4) stream was reacted over Ru/TiO_2 (curves a, c) and Ru/Al_2O_3 (curve b) catalysts at 575 K (curves a, b) and 625 K (curve c).

3.1.2. Continuous flow

The activity of the low temperature (< 500 K) H_2-reduced catalysts was found to fall with time when the $CO + H_2$ reaction was studied in flow mode at reaction temperatures below 525 K. The activity at the higher reaction temperatures was, however, found to remain stable during various hours of test time. The H_2 pretreatment effect was therefore evaluated at the reaction temperatures of 525 K and above. Fig. 4 presents the activity of the two titania and alumina supported catalysts for the reaction of $CO + H_2$ (1:4) stream at the typical temperatures of 575 (curves a, b) and 625 (curve c), as a function of H_2 pretreatment in range 500–900 K. As seen in these data, the methane yield at a reaction temperature of 575 K decreases sharply at the H_2 reduction temperatures above 600 K, in case of both the titania (Fig. 4a) and the alumina (Fig. 4b) supported ruthenium. On the other hand, the activity at a reaction temperature of 625 K was found to be unaffected of the high temperature H_2 pretreatment given to a catalyst (Fig. 4c).

3.2. Infrared spectra of adsorbed CO

3.2.1. Ru/TiO_2 catalyst

Spectra a and b of Fig. 5 show the vibrational bands developed on exposure of two titania

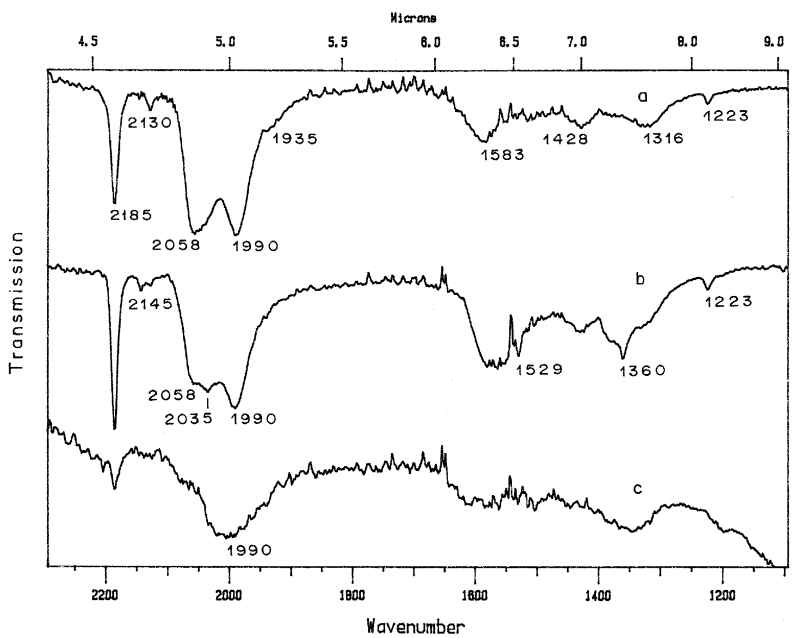

Fig. 5. IR spectra of 575K H_2 reduced $Ru(2.2\%)/TiO_2$ (a) and $Ru(4.3\%)/TiO_2$ (b) catalysts when exposed at room temperaturee to 100 Torr CO. Spectrum (c) shows the vibrational bands developed on $Ru(4.3\%)/TiO_2$ sample after CO adsorption at 375 K.

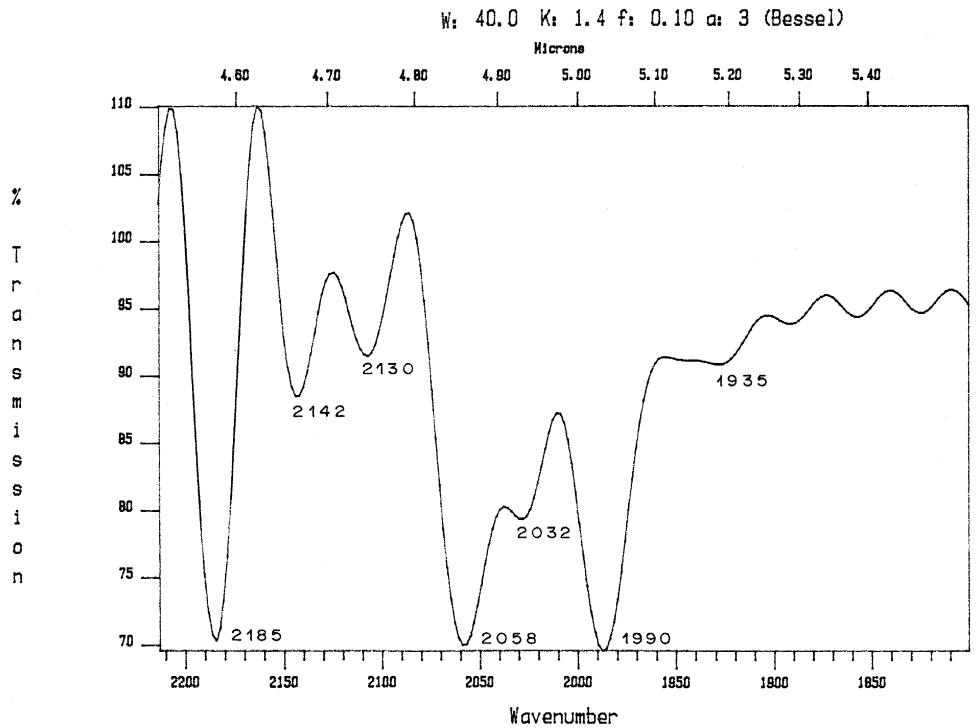

Fig. 6. Deconvolution of C–O stretch bands in spectrum a of Fig. 5.

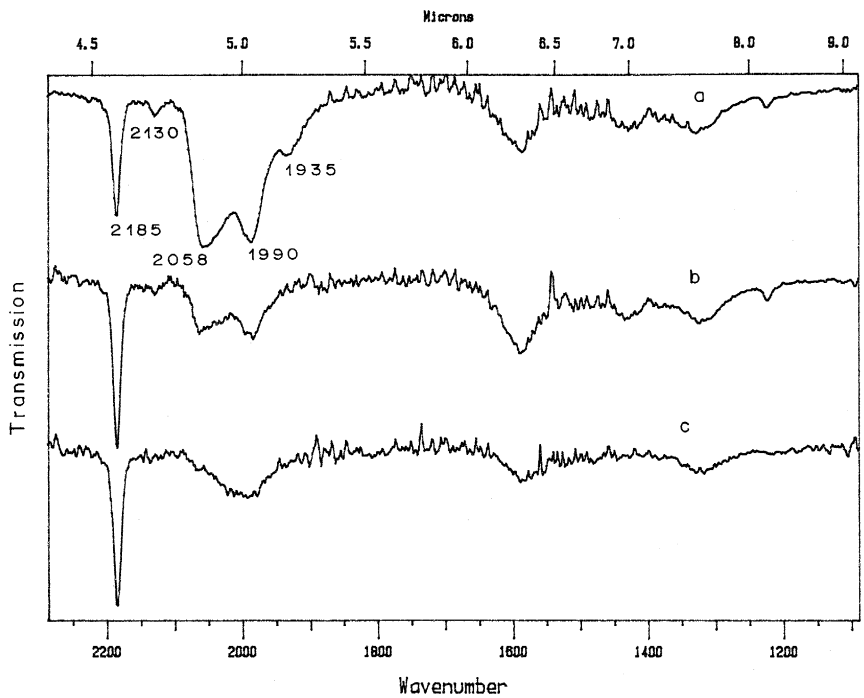

Fig. 7. The vibrational bands developed over Ru(2.2%)/TiO_2 catalyst after room temperature adsorption of 100 Torr CO when the catalyst was reduced in H_2 at different temperatures. (a) 675 K, (b) 725 K, (c) 775 K.

supported Ru catalysts to 100 Torr of CO. As mentioned in Section 2, data in Fig. 5 represent the difference spectra obtained after subtracting the IR bands due to gaseous CO present in the cell. Also, as brought out in our earlier publications [13–15], the broad and overlapping C–O stretch vibrational bands may be better resolved using a deconvolution program. A deconvolution of CO bands in Fig. 5a is presented in Fig. 6 which shows the presence of at least six individual vibrational bands appearing at around 2142, 2130, 2058, 2035, 1990 and 1935 cm^{-1}.

Spectrum b in Fig. 5 clearly shows the presence of a band at 2035 cm^{-1} which overlapped with 2058 cm^{-1} band in Fig. 5a. Evacuation of the cell at temperatures in the range of 300–400 K resulted in the removal of almost all the bands except one broad band appearing at 1990 cm^{-1}. A similar effect was observed when the CO was dosed over Ru/TiO_2 at elevated temperatures. As an example, spectrum c in Fig. 5 shows the vibrational bands observed during exposure of $Ru(4.3\%)/TiO_2$ to 100 Torr CO at 375 K. Further increase in the CO exposure temperature resulted in the reduced intensity of 1990 cm^{-1} band though the shift in its frequency was only marginal.

The hydrogen pretreatment given to a sample at higher temperatures had considerable effect on the νCO bands in Fig. 5. Fig. 7 presents these data, where spectra a–c show the vibrational bands formed during exposure of $Ru(2.2\%)/TiO_2$ to 100 Torr CO after hydrogen reduction at 675, 725 and 775 K, respectively. A comparison with Fig. 5a shows that the H_2 pretreatment at temperatures up to 675 K had practically no influence on the frequency and the intensity of C–O stretch bands (Fig. 7a). The reduction at higher temperatures led to the progressive removal of all the bands, the effect being more pronounced on the νCO bands appearing at the frequency greater than 1990 cm^{-1} (Fig. 7b). Only one broad band centred at ca. 1990 cm^{-1} was seen after CO exposure over

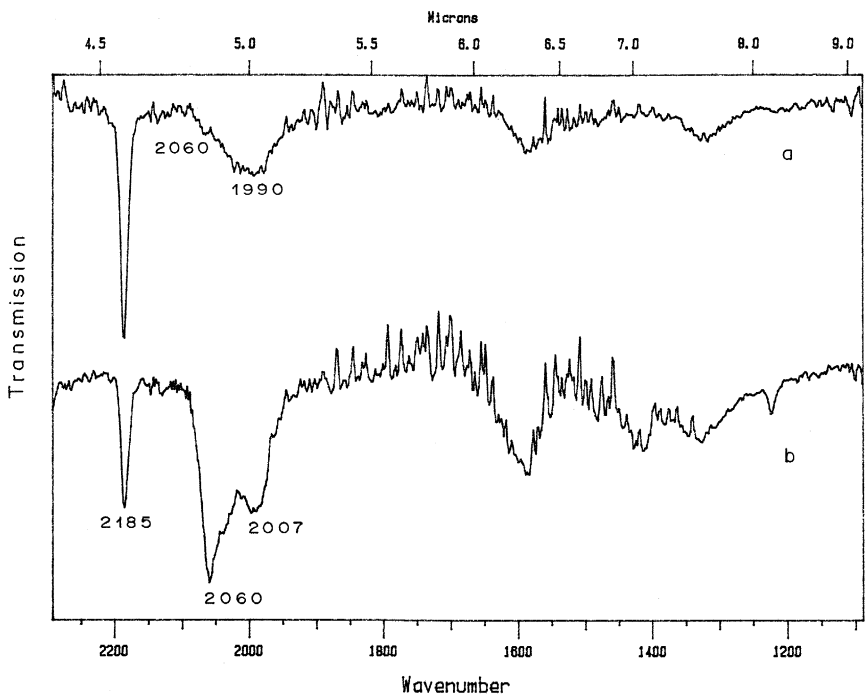

Fig. 8. Effect of reoxidation (475 K, 2 h) followed by H_2 activation (500 K, 2 h) on the vibrational bands formed over 775 K reduced $Ru(2\%)/TiO_2$ catalyst after room temperature exposure to 100 Torr CO (spectrum b). Spectrum (a) shows the comparative data for a 775 K reduced catalyst without a reoxidation treatment.

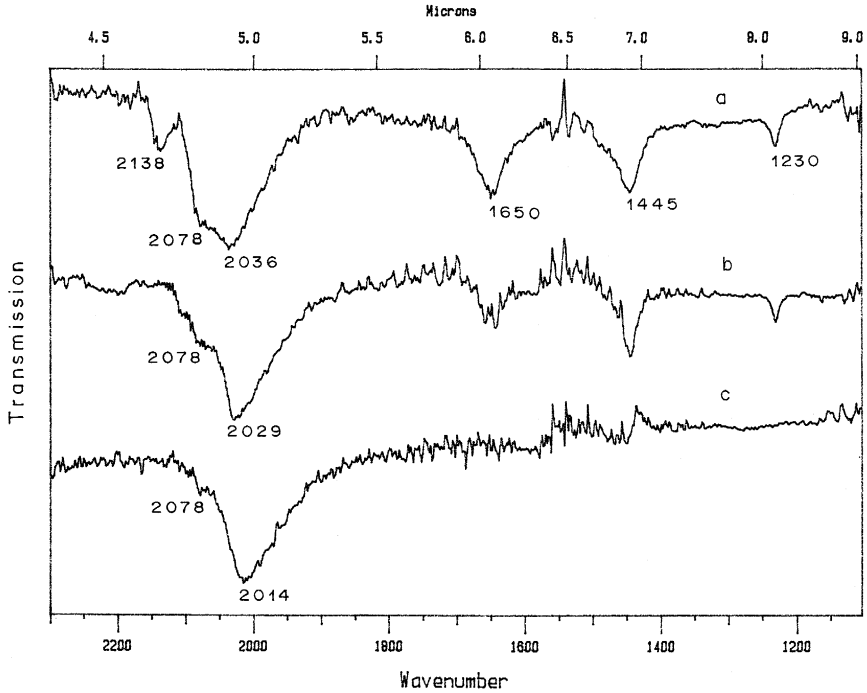

Fig. 9. IR spectra of a Ru(4.5%)/Al_2O_3 catalyst exposed to 100 Torr CO at (a) 300 K, (b) 375 K and (c) 475 K.

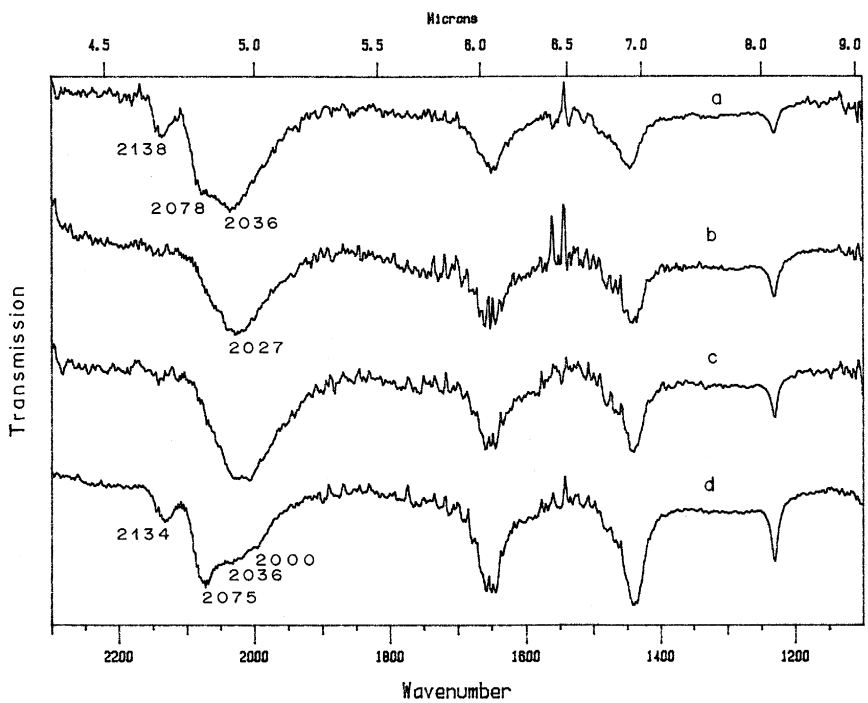

Fig. 10. Spectra a–c show the vibrational bands developed over Ru(4.5%)/Al_2O_3 catalyst surface after exposure to 100 Torr CO at 300 K as a function of catalyst pretreatments under H_2 at different temperatures. (a) 475 K, (b) 675 K and (c) 775 K. Spectrum d shows the corresponding data when a 775 K reduced catalyst was subjected to oxidation (475 K, 2 h) followed by H_2 activation (500 K, 2 h) before CO exposure.

Ru/TiO_2 samples reduced at a temperature above 775 K (Fig. 7c). Also, almost negligible CO adsorption occurred when the hydrogen pretreatment temperature was more than 850 K.

When a high temperature ($>$ 775 K) reduced Ru/TiO_2 sample was heated in situ under oxygen (525 K, 2 h), the sample transmittance improved and it also regained its CO adsorption properties. As shown in the data of Fig. 8b, strong νCO bands at 2035 and 2060 cm^{-1} and a weak band at 2135 cm^{-1} reappeared when a 775 K reduced $Ru(2.2\%)/TiO_2$ sample was subjected to the above mentioned O_2 and H_2 pretreatments (cf. Fig. 8a).

3.2.2. Ru/Al_2O_3 catalyst

The CO exposure at 300 K over 475 K reduced Ru/Al_2O_3 gave rise to at least four CO stretch vibrational bands at 2138, 2078, 2036 and 2000 cm^{-1}. The main peak at 2036 cm^{-1} exhibited considerable increase in the intensity and showed a blue shift with the increase of CO pressure in the IR cell; its frequency shifting from a value of 2019 to 2040 cm^{-1} for an increase in the CO pressure from 1 to 200 Torr. The frequency of other bands, however, remained almost unchanged. On raising the CO exposure temperature, the higher frequency bands were removed progressively, whereas the 2036 cm^{-1} band showed a red shift. These data are given in Fig. 9 for three different catalyst temperatures in 300–400 K range.

Fig. 10 presents the effect of H_2 pretreatment on the νCO bands developed over Ru/Al_2O_3 catalyst during 100 Torr CO exposure at 300 K. As seen in Fig. 10b and Fig. 10c, the intensity of 2138 and 2078 cm^{-1} bands was reduced drastically for the H_2 pretreatment temperatures of 675 and 775 K. The intensity of 2036 cm^{-1} band was reduced by ca. 25% (as evaluated by absorbance value) and its frequency shifted to a lower value of ca. 2025 cm^{-1} as a result of high temperature reduction (Fig. 10c). The intensity of this band was reduced further on raising the reduction temperature to 875 K.

The reoxidation (525 K, 2 h) of a 875 K reduced Ru/Al_2O_3 catalyst followed by H_2 activation (500 K, 2 h) resulted in the restoration of all the νCO bands, as shown in the spectrum d of Fig. 10.

4. Discussion

The frequencies of C–O stretch bands developed over supported noble metal catalysts during exposure to carbon monoxide are known to depend upon various factors, such as the nature, dispersion, oxidation state, and the crystallographic phase of exposed metal, in addition to the nature of support, surface coverage and the reaction conditions. These bands have been widely reviewed [3,7,15] and only salient features are therefore mentioned here. There is an unanimity of view in the assignment of 2185 cm^{-1} band to physisorbed CO while the νCO bands in 1950–2050 cm^{-1} region are normally attributed to the linearly bonded CO. A number of infrared and chemisorption studies on the CO adsorption over group Vlll metals have also shown that the formation of the linearly bonded CO adstates is promoted by the metal crystallites of large size, while the well dispersed metal sites are responsible to the formation of multicarbonyl ($Ru(CO)_n$) type surface species [22–24]. The IR bands in 2000–2050 cm^{-1} region are therefore identified with the Ru_x CO species, where x is the number of the metal atoms in a cluster [3,25]. Different views have, however, been expressed on the origin of νCO bands in 2075–2145 cm^{-1} region. For instance, the bands appearing at 2135 and 2080 cm^{-1} were initially assigned to C–O stretching vibration of CO adsorbed on a surface oxide and CO adsorbed on a Ru atom perturbed by a nearby oxygen atom, respectively [2]. Robbins [4] and Chen et al. [10] have more recently used isotopically labelled CO to show that the 2140 and 2085 cm^{-1} bands were coupled vibrations of an $Ru(CO)_n$ ($n = 2$ or 3) species. Similarly, a band at ca. 2132–2135 cm^{-1} in conjunction with 2085 cm^{-1} band is assigned to a multicarbonyl

Table 2
C–O Stretch bands observed during room temperature adsorption of CO over Ru/TiO_2 and Ru/Al_2O_3 catalysts

Frequency cm^{-1}	Assignment
2185	Physisorbed CO
2145	$Ru^{\circ}–(CO)_n$
2130–2135	$Ru^{\delta+}–(CO)_n$
2078	$Ru^{\circ}–(CO)_n$ and $Ru^{\delta+}–(CO)_n$
2058	$Ru_x–(CO)$
2035	$Ru' \begin{matrix} CO \\ \diagdown \\ O \end{matrix}$
1990	$Ru'_x–(CO)$
1935	$Ru''_x–(CO)$ or $(Ru)_2–CO$

species bonded to Ru of a higher oxidation state [8,13,15]. With this in view, the possible assignments of some of the CO bands in Fig. 8, Fig. 9, and Fig. 10 are given in Table 2 , where Ru, Ru′ and Ru″ represent the metal sites of varying morphological/crystallographic nature [20], which may marginally affect the mode of CO bonding.

Recent infrared studies have demonstrated that a long-duration low-temperature CO exposure given to supported Ru and Rh catalysts resulted in the progressive growth of $M^{\delta+}(CO)_n$ species, which has been attributed to the oxidative disruption of the metal clusters [3,25–28]. The rate of this oxidative disruption is found to depend on the size of Ru_x particles. On the other hand, a reverse process occurred at the higher temperatures (> 500 K), when the reductive agglomeration of $Ru^{\delta+}$ sites gave rise to the reformation of Ru_x clusters and the size of Ru_x clusters depends on the reduction temperature [3,28]. The relative intensities of different IR bands in Fig. 7 and Fig. 9 therefore reveal the agglomeration of the metal particles over catalyst surface as a result of high temperature reduction and hence in the growth of the Ru_x CO type species. This is supported by the results of our SEM study showing substantial metal segregation over Ru/TiO_2 surface as a result of high temperature reduction [21].

The loss in catalytic activity (particularly at the reaction temperatures below 500 K) as a function of H_2 pretreatment (Fig. 1 and Fig. 2), shows a strong correspondence with the progressive removal of the high frequency bands (2050–2145 cm^{-1}) under identical pretreatment conditions (Fig. 7 and Fig. 10). For instance, the reduction at temperatures up to 675 K had practically no effect on the vibrational bands developed during CO adsorption over Ru/TiO_2 catalyst (Fig. 7a). On the other hand, the catalyst reduction at temperatures above 675 K led to the reduced intensity of almost all the bands, the effect being more pronounced on the νCO bands appearing at the frequencies greater than 2000 cm^{-1} (Fig. 7b and Fig. 7c). This finds parallelism with the progressive loss of catalytic activity when a Ru/TiO_2 catalyst was H_2 pretreated at temperatures above 675 K (Fig. 1 and Fig. 4). A similar correlation may be noticed in the data for Ru/Al_2O_3 catalyst (Fig. 2, Fig. 4 and Fig. 10a–c).

Since the pretreatment mentioned above influenced the catalyst activity only at lower reaction temperatures while the activity at higher temperatures remained almost unaffected, we may conclude that the reaction routes governing the catalyst activity in the two temperature ranges may be different. We may also infer that the $(CO)_{ad}$ modes giving rise to the vibrational bands in higher frequency region are particularly responsible to the low temperature catalytic activity. Earlier studies reported from this laboratory [15,29] using a better dispersed Ru/TiO_2 catalyst have shown that the CO methanation at low temperatures (< 475 K) occurs via multicarbonyl $\rightarrow$ monocarbonyl $\rightarrow$ Ru–C or multicarbonyl $\rightarrow$ methylene groups $\rightarrow$ hydrocarbon route, where the excited CO^* species formed during dissociation of $Ru(CO)_n$ play an important role. On the other hand, the disproportionation of the linearly adsorbed CO (Boudouard reaction) is shown to govern the CO methanation at higher reaction temperatures. The results of the present study support these views.

The effect of metal particle size on the activity of transition metal catalysts is a widely

investigated phenomenon, as is reviewed in [30]. The studies of Dalla Betta et al. [31] and Elliott and Lunsford [32] have shown that the CO methanation over Ru/Al_2O_3 and Ru/Zeolite-Y was structure insensitive at the reaction temperature of 555 K. On the other hand, this reaction has been shown to be antipathetic structure sensitive when the Ru/SiO_2 and Ru/Al_2O_3 catalysts were used in the temperature range of 475–525 K [6,33]. In agreement with this, the results of present study show that only some of the $(CO)_{ad}$ modes are structure sensitive and these are the modes which are responsible for the catalyst activity at lower reaction temperatures. Data in Fig. 5 also support these inferences.

The data in Fig. 5c and Fig. 9 show that the high frequency bands were unstable and were removed easily on evacuation or at the elevated sample temperatures. The formation of these bands was also inhibited by the S-deposition on catalyst surface [20] which showed a parallelism with the loss of catalyst activity for the CO adsorption and low temperature methanation.

The crucial role of metal dispersion in CO adsorption behaviour is also reflected in the data of Fig. 8b and Fig. 10d which show that some of the high frequency bands reappeared when a high temperature reduced catalyst was oxidized followed by an activation in H_2 at lower temperature. This finds parallelism with the observed restoration of the catalyst activity after these pretreatments. Similar oxidation-reduction treatment is known to result in the re-dispersion of metal agglomerates [21]. This also tends to support the concept of the oxidative disruption of metal clusters which result in the reformation of $M^{\delta+}(CO)_n$ species [3,25–28].

The results discussed above thus lead to the following conclusions. The mode of adsorption over transition metal surface depends on the metal dispersion and it decides the stability and the reactivity of the adsorbed CO molecules. The $(CO)_{ad}$ modes giving rise to νCO bands in 2050–2145 cm^{-1} region (Table 2) are unstable and are formed only over highly dispersed metal surfaces. The CO_{ad} species in this form are reactive to H_2 at lower temperatures giving rise to methane formation via transient $(-CH_2)_n$ moieties as mentioned above. On the other hand, the $(CO)_{ad}$ species responsible for the vibrational bands at ca. 2000 cm^{-1} or below are more stable and are by and large insensitive to the metal particle size or to the presence of adsorbates such as sulphur [20]. These species hydrogenate to give methane at higher reaction temperatures via disproportionation of CO and the formation of 'active' carbon intermediates. The temperature dependent C_2H_6 yields in Fig. 3 show that the formation of higher hydrocarbons may also depend on the metal dispersion and the nature of $(CO)_{ad}$ species formed at a particular temperature. While the $Ru(CO)_n$ species may give rise to higher hydrocarbons at lower reaction temperatures (Fig. 3, curves a–c), the isolated Ru–CO groups formed over poorly dispersed metal sites may give these products only at the elevated reaction temperatures (Fig. 3d and Fig. 3e). A better understanding of these aspects, however, needs further investigations.

Acknowledgements

The authors thank a referee for his helpful comments.

References

[1] R.A. Dalla Betta, J. Phys. Chem. 79 (1975) 2519.
[2] M.F. Brown and R.D. Gonzalez, J. Phys. Chem. 80 (1976) 1731.
[3] F. Solymosi and J. Rasko, J. Catal. 115 (1989) 107.
[4] J.L. Robbins, J. Catal. 115 (1989) 120.
[5] I. Mochida, H. Fugitsu and N. Jkeyama, J. Chem. Soc., Faraday Trans. 83 (1987) 1427.
[6] C.S. Kellner and A.T. Bell, J. Catal. 75 (1982) 251.
[7] G.H. Yokomizo, C. Louis and A.T. Bell, J. Catal. 120 (1989) 1.
[8] E. Guglielminotti and G.C. Bond, J. Chem. Soc., Faraday Trans. 86 (1990) 979.
[9] M.W. McQuire and C.H. Rochester, J. Catal. 141 (1993) 355.

[10] H.W. Chen, Z. Zhong and J.M. White, J. Catal. 90 (1984) 119.
[11] H. Yamasaki, Y. Kobori, S. Naito, T. Onishi and K. Tamaru, J. Chem. Soc., Farady Trans. 1, 77 (1981) 2913.
[12] F. Solymosi and H. Knozinger, J. Chem. Soc., Faraday Trans. 86 (1990) 389.
[13] N.M. Gupta, V.S. Kamble, R.M. Iyer, K.R. Thampi and M. Graetzel, J. Catal. 137 (1992) 473.
[14] N.M. Gupta, V.S. Kamble, K.R. Thampi and M. Graetzel, Catal. Lett. 21 (1993) 245.
[15] N.M. Gupta, V.S. Kamble, V.B. Kartha, K.R. Thampi and M. Graetzel, J. Catal. 146 (1994) 173.
[16] M.W. Balakos, S.S.C. Chuang, G. Srinivas and M.A. Brundage, J. Catal. 157 (1995) 51.
[17] S.J. Tauster, in: Strong Metal–Support Interactions, eds. R.T.K. Baker, S.J. Tauster and J.A. Dumesic, (Am. Chem. Soc., Washington, DC, 1986), Ch. 1, p. 1.
[18] R. Burch, in: Hydrogen Effects in Catalysis, eds. Z. Papal and P.G. Menon, (Marcel Dekker, New York, 1988), p. 347.
[19] G.L. Haller and D.E. Resasco, in: Advances in Catalysis, Vol. 36, eds. D.D. Eley, H. Pines and P.B. Weisz (Academic Press, New York, 1989), p. 36.
[20] V.S. Kamble, V.P. Londhe, N.M. Gupta, K.R. Thampi and M. Graetzel, J. Catal. 158 (1996) 427.
[21] V.P. Londhe, K.K. Kutty, B.M. Pande and N.M. Gupta, unpublished work.
[22] C.H. Bartholomew and R.B. Pannell, J. Catal. 65 (1980) 390.
[23] D.J.C. Yates, L.L. Murrell and E.B. Prestridge, J. Catal. 57 (1979) 41.
[24] H.C. Yao, S. Japar and M. Shelef, J. Catal. 50 (1977) 407.
[25] V.L. Kunznetsov, A.T. Bell and Y.J. Yermakov, J. Catal. 65 (1980) 374.
[26] F. Solymosi and H. Knozinger, J. Chem. Soc., Faraday Tras. 86 (1990) 389.
[27] F. Solymosi and M. Pasztor, J. Phys. Chem. 90 (1986) 5312.
[28] T. Mizushima, K. Tohji, Y. Udagawa and A. Ueno, J. Phys. Chem. 94 (1990) 4980.
[29] N.M. Gupta, K.R. Thampi, V.S. Kamble, V.P. Londhe, H. Oz and M. Gratzel, Ind. J. Chem. 33A (1994) 365.
[30] M. Che and C.O. Bennettt, in: Advances in Catalysis, Vol. 36, D.D. Eley, H. Pines and P.B. Weisz (Academic Press, New York, 1989), p. 55.
[31] R.A. Dalla Betta, A.G. Piken and M. Shelef, J. Catal. 35 (1974) 54.
[32] D.J. Elliott and J.H. Lunsford, J. Catal. 57 (1979) 11.
[33] D.L. King, J. Catal. 51 (1978) 386.